ELSEVIER

Available online at www.sciencedirect.com

SCIENCE DIRECT®

Journal of Nuclear Materials 344 (2005) 8–12

journal of nuclear materials

www.elsevier.com/locate/jnucmat

Thermodynamics of water sorption on PuO_2: Consequences for oxide storage and solubility

John M. Haschke *

Actinide Science Consulting, 11003 Willow Bend Drive, Waco, TX 76712, USA

Abstract

Gibbs energies for sorption of water on plutonium dioxide are derived from equilibrium pressure-surface composition data at 298–358 K. Sorption occurs in well-defined initial steps that form variable-composition surface phases by successive addition of H_2O layers and ultimately in a continuum. ΔG^0 values vary from −24.6 to −16.1 kJ per mol H_2O as y in the initial $PuO_{2-y}(OH)_{2y}$ product increases from 0 to 1 and from −16.1 to −11.0 kJ per mol H_2O during formation of $PuO(OH)_2 \cdot nH_2O$ (n = 0 to 1) in the second step. These results are consistent with dissociative chemisorption at 298 K and with desorption near 575 K. Gibbs energies for higher sorption steps at 298 K asymptotically approach ΔG^0 for condensation of water (−8.56 kJ mol^{-1}) and are consistent with reversible physisorption. Respective ΔG^0_{f298} and ΔH^0_{f298} are −1247 and −1338 kJ mol^{-1} for $PuO(OH)_2$; corresponding values are −1488 and −1608 kJ mol^{-1} for $PuO(OH)_2 \cdot H_2O$. Results do not support claims that all water is reversibly desorbed at 350–500 K or that dioxide solubility is enhanced by formation of $Pu(OH)_4$(am) on the surface.

1. Introduction

Sorption of water on crystalline PuO_2 alters chemical behavior of the oxide and oxide-coated metal in technologically important ways [1]. Amounts of water sorbed on high-surface-area oxide are sufficient to generate excessively high H_2 pressures in storage containers [2,3]. Formation of surface hydroxide is identified as a key step in catalytic cycles that enhance Pu corrosion in moist air [4] and promote formation of a high-composition oxide, PuO_{2+x}, and H_2 [5]. A higher-than-expected PuO_2 solubility is attributed to formation of surface hydroxide [6] similar to the more soluble amorphous hydrous oxide, $Pu(OH)_4$ (am), formed by precipitation of aqueous Pu(IV).

Gravimetric and spectroscopic data show that water readily sorbs on PuO_2 at room temperature and low humidity [7–10]. Dissociative chemisorption of H_2O as hydroxide during an initial step and formation of a variable-composition oxide hydroxide phase, $PuO_{2-y}(OH)_{2y}$ (y = 0 to 1), at low water pressures (P_{H_2O} < 1.5 mbar) is proposed [10]. Sorption of a second H_2O layer is complete at water pressures near 10 mbar and up to 8 additional layers of molecular H_2O adsorb as P_{H_2O} increases to saturation. Desorption of H_2O in the 370–425 K and the 570–625 K ranges with respective activation energies of 84 and 285 kJ mol^{-1} is followed by an additional mass loss at 1000–1200 K [11]. However, closed-system measurements show reversible adsorption–desorption of all water in the 350–500 K range with desorption enthalpies of 51–44 kJ mol^{-1} for

---

* Tel.: +1 254 399 0740; fax: +1 254 399 8876.
E-mail address: johnhaschke@msn.com

0022-3115/$ - see front matter © 2005 Elsevier B.V. All rights reserved.
doi:10.1016/j.jnucmat.2005.04.007

coverages of one to several H_2O layers [12]. Enthalpies of H_2O adsorption and desorption are considered equal because a non-activated desorption process is assumed for reversibly bound water.

Thermodynamic properties of variable-composition surface phases formed during sorption of water on plutonium dioxide are derived in an effort to more adequately describe the sorption process. Results are applied in evaluating thermal desorption and in assessing effects of surface phases on oxide solubility.

2. Data and methods

Thermodynamic evaluation is based on gravimetric measurements during equilibration of PuO_2 with H_2O vapor [8] and with low-humidity air [10,13]. Weapons-grade (~94% ^{239}Pu) oxides prepared from metal or oxalate were calcined at 975–1275 K prior to BET determinations of specific surface areas. Mass changes were measured during exposure of oxide samples to H_2O vapor at 298 ± 5, 323 ± 2, and 358 ± 2 K and fixed pressures, P_{H_2O}, of 0.1–30 mbar [8,10]. Isotherms in Fig. 1 describe the dependencies of equilibrium concentrations of sorbed water, $[H_2O]_s$ in mg m^{-2}, on P_{H_2O} and indicate the uncertainty in measurements. Surface compositions vary with increasing P_{H_2O} along all isotherms.

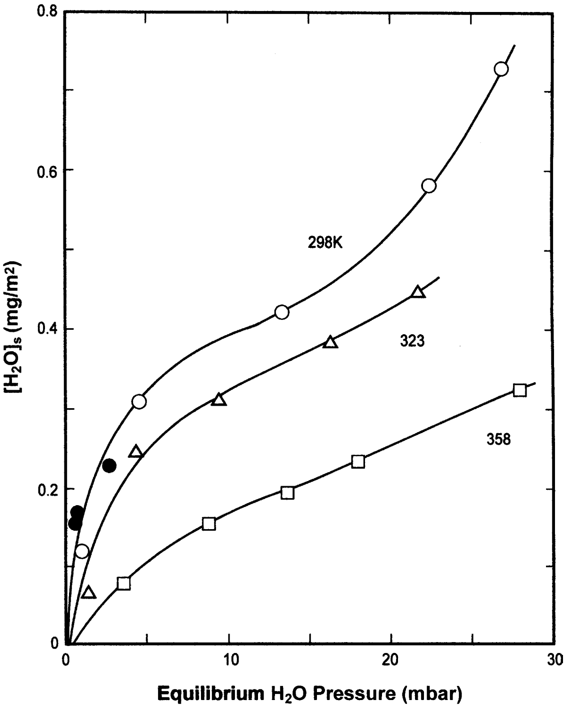

Fig. 1. Isotherms for sorption of water on PuO_2(cr). Surface concentrations of sorbed water, $[H_2O]_s$ and corresponding equilibrium water pressures at 298 K (○), 323 K (△), and 358 K (□) are from [8] (open symbols) and [10] (solid symbols).

Gibbs energies for sorption of water on PuO_2 are derived using integral methods. As defined by $-RT\ln K$ with $K = (P_{H_2O})^{-1}$, partial molar Gibbs energies, $\underline{G}_T$, for isothermal sorption of water on oxide are derived as a function of $[H_2O]_s$ using curves in Fig. 1. ΔG_T^0 values determined by integration of $\underline{G}_T$-composition data for successive sorption reactions are correlated with temperature to define enthalpies and entropies of sorption. Thermodynamic properties of products are derived using results and reference data.

3. Results and discussion

Derived $\underline{G}_T$-composition isotherms (Table 1) are continuous functions comprised of successive linear segments that each involve a change in $[H_2O]_s$ of 0.21 mg m^{-2}, the amount of water required for monolayer coverage of the dioxide surface [10,12]. Agreement of the mass change for each $\underline{G}_T$-composition step with the theoretical value shows that sorption of H_2O on PuO_2 occurs in discrete sequential steps that each correspond to addition of one H_2O layer. Dependence of $\underline{G}_T$ on composition within each step implies that ΔG_T^0 of sorption varies continuously as each layer forms; differences in these slopes imply that each step is a unique equilibrium-controlled sorption reaction.

Formulation of step-wise sorption reactions is based on the 1:1 association of H_2O and Pu in the layer and on sorption of 0.21 mg m^{-2} during each step [10]. The stoichiometric ratio and reflectance FTIR data showing absorption peaks for hydroxide [10] are consistent with dissociative chemisorption of water during Step 1:

$$PuO_2(cr) + yH_2O(g) \rightarrow PuO_{2-y}(OH)_{2y}(ads,\ surf). \quad (1)$$

The surface composition varies from PuO_2 for $y = 0$ to $PuO(OH)_2$ for $y = 1$ at monolayer completion. If reduced oxide is formed during calcination, complete transformation to Pu(IV) oxide is expected before Eq. (1) initiates because ΔG^0 for oxidation of $Pu_2O_3(s)$ to $PuO_2(s)$ by $H_2O(g)$ at 298 K and 0.1 mbar pressure -164 kJ mol^{-1} [14].

Subsequent sorption of water occurs by progressive change of surface stoichiometry in discrete steps. Step 2 is described as follows with values of n varying from 0 to 1:

$$PuO(OH)_2(ads,\ surf) + nH_2O(g) \rightarrow PuO(OH)_2 \cdot nH_2O(ads,\ surf). \quad (2)$$

The product is identified as a hydrate because water forms during desorption [11], but formulation as $PuO_{1-n}(OH)_{2+2n}$ (ads, surf) with $Pu(OH)_4$ as the

Table 1
Least-squares lines defining linear segments of $\underline{G}_T$-composition isotherms derived from $[H_2O]_s$-P_{H_2O} data in Fig. 1[a]

Composition range		298 K		323 K		358 K	
$[H_2O]_s$ (mg m^{-2})	y, n, n', or n''	A (kJ)	B (kJ mol^{-1})	A (kJ)	B (kJ mol^{-1})	A (kJ)	B (kJ mol^{-1})
0.00–0.21	$y = 0 - 1$	−24.63 ± 0.51	8.47 ± 0.74	−21.17 ± 0.37	5.94 ± 0.54	−19.79 ± 0.17	7.18 ± 0.25
0.21–0.42	$n = 0 - 1$	−16.11 ± 0.04	4.94 ± 0.06	−15.19 ± 0.09	4.37 ± 0.14	−12.41 ± 0.05	2.85 ± 0.10
0.42–0.63	$n' = 0 - 1$	−10.87 ± 0.22	1.70 ± 0.36	–	–	–	–
>0.63	$n''>0$	9.33	1.42	–	–	–	–

[a] In all composition ranges, $\underline{G}_T$ (kJ) = $A + By$ (or n, n', or n'') where y refers to Eq. (1) (or where n refers to Eq. (2), n' to Eq. (3) or n'' to Eq. (4)).

terminal product is an alternative. A third step resolved only at 298 K is attributed to sorption of molecular H_2O:

$$\begin{aligned} &PuO(OH)_2 \cdot H_2O(\text{ads, surf}) + n'H_2O(g) \\ &\quad \rightarrow PuO(OH)_2 \cdot (1+n')H_2O(\text{ads, surf}). \end{aligned} \tag{3}$$

Termination of Step 3 at $n' = 1$ is marked by onset of a fourth reaction:

$$\begin{aligned} &PuO(OH)_2 \cdot 2H_2O(\text{ads, surf}) + n''H_2O(g) \\ &\quad \rightarrow PuO(OH)_2 \cdot (2+n'')H_2O(\text{ads, surf}). \end{aligned} \tag{4}$$

Definition of Step 4 is limited by lack of data for $[H_2O]_s > 0.63$ mg m^{-2}.

Values of ΔG^0_T for Eqs. (1)–(4) at selected extents of reaction (Table 2) are used with reference data for PuO_2(cr) and H_2O(g) [14] to derive accompanying Gibbs energies of formation for $PuO_{2-y}(OH)_{2y}$ and $PuO(OH)_2 \cdot nH_2O$. ΔH^0 and ΔS^0 values for Eqs. (1) and (2) (Table 3) are defined by least-squares regression analysis of the ΔG^0–T data. The results are used with reference data [14] to determine accompanying ΔH^0_f and S^0 values for PuO_{2-y} $(OH)_{2y}$ and $PuO(OH)_2 \cdot nH_2O$. Derivation of enthalpy and entropy results for Eqs. (3) and (4) is precluded by lack of data for high temperatures.

Interpretation is aided by examining the composition dependence of standard Gibbs energies for sorption as y, n, n' and n'' progressively increase from 0 to 1 in successive steps. As shown by partial molar data (Table 1), ΔG^0_{298} values per mole of H_2O for Step 1 increase from −24.6 to −16.1 kJ mol^{-1} as y increases from 0 to 1. Respective ranges for Steps 2–4 are, −16.1 to −10.9, −10.9 to −9.3, and −9.3 to −8.8 kJ mol^{-1}. Contrary to the conclusions of Paffett et al. [12], equilibrium results confirm kinetic observations [10] by showing up to four distinct water layers that sorb sequentially in Steps 1–4. The magnitudes of ΔG^0_{298} are consistent with

Table 2
Derived Gibbs energies for sorption of water on PuO_2 and Gibbs energies of formation for resulting surface phases as functions of temperature and composition

y or n	ΔG^0_T[a] Eq. (1) (kJ mol^{-1})	ΔG^0_{fT}[b] $PuO_{2-y}(OH)_{2y}$ (kJ mol^{-1})	ΔG^0_T[a] Eq. (2) (kJ mol^{-1})	ΔG^0_{fT}[b] $PuO(OH)_2 \cdot nH_2O$ (kJ mol^{-1})	ΔG^0_T[a] Eq. (3) (kJ mol^{-1})	ΔG^0_T[a] Eq. (4) (kJ mol^{-1})
T = 298 K						
0.25	−5.90	−1061.1 ± 1.0	−3.87	−1308.0 ± 1.3	−2.67	−2.26
0.50	−11.25	−1123.6 ± 2.2	−7.44	−1368.8 ± 2.6	−5.22	−4.50
0.75	−16.08	−1185.6 ± 3.1	−10.69	−1429.2 ± 3.4	−7.67	(−6.7)[c]
1.00	−20.39	−1247.0 ± 4.0	−13.64	−1488.0 ± 4.4	−10.02	(−8.9)[c]
T = 323 K						
0.25	−5.10	−1055.6 ± 1.0	−3.66	−1299.8 ± 1.1	–	–
0.50	−9.84	−1117.3 ± 1.9	−7.05	−1360.1 ± 1.8	–	–
0.75	−14.20	−1178.4 ± 2.1	−10.16	−1420.0 ± 2.5	–	–
1.00	−18.20	−1239.3 ± 3.4	−13.00	−1479.8 ± 3.4	–	–
T = 358 K						
0.25	−4.72	−1049.0 ± 0.9	−3.19	−1289.3 ± 1.2	–	–
0.50	−9.00	−1109.7 ± 1.5	−5.85	−1348.4 ± 1.7	–	–
0.75	−12.82	−1170.0 ± 1.9	−8.51	−1407.5 ± 2.5	–	–
1.00	−16.20	−1229.9 ± 2.8	−10.99	−1466.5 ± 3.3	–	–

[a] Estimated standard errors in ΔG^0_T for Eqs. (1)–(4) (5%, 10% and 15% of the measured value, respectively) include a possible factor-of-two error in the pressure-composition data (Fig. 1).

[b] Estimated errors (95% confidence) in ΔG^0_{fT} are cumulative values based on uncertainties in $\underline{G}_T$-composition data and reference data.

[c] Value estimated by linear extrapolation based on constant incremental change determined at lower composition.

Table 3
Enthalpies and entropies for the first and second steps of water sorption on PuO_2 and derived enthalpies of formation and entropies of resulting surface phases as functions of composition

y	ΔH^{0a}Eq. (1) (kJ mol^{-1})	ΔS^{0a}Eq. (1) (J K^{-1} mol^{-1})	ΔH_f^{0b} $PuO(OH)_2 \cdot nH_2O$ (kJ mol^{-1})	S^{0b} $PuO(OH)_2 \cdot nH_2O$ (J K^{-1} mol^{-1})
Eq. (1)				
0.25	−11.43 ± 1.8	−18.98 ± 5.7	−1127.7 ± 5.8	94 ± 11
0.50	−22.02 ± 2.2	−36.72 ± 8.8	−1189.7 ± 7.8	124 ± 18
0.75	−31.79 ± 3.2	−53.36 ± 9.8	−1269.0 ± 8.6	154 ± 20
1.00	−40.78 ± 2.8	−68.99 ± 8.4	−1338.4 ± 7.9	186 ± 17
n	ΔH^{0a} Eq. (2) (kJ mol^{-1})	ΔS^{0a} Eq. (2) (J K^{-1} mol^{-1})	ΔH_f^{0b} $PuO_{2-y}(OH)_{2y}$ (kJ mol^{-1})	S^{0b} $PuO_{2-y}(OH)_{2y}$ (J K^{-1} mol^{-1})
Eq. (2)				
0.25	−7.33 ± 0.4	−11.50 ± 1.4	−1406.2 ± 6.1	222 ± 13
0.50	−15.57 ± 1.7	−26.93 ± 5.0	−1474.9 ± 8.3	255 ± 20
0.75	−21.89 ± 3.6	−37.10 ± 7.2	−1541.7 ± 9.2	291 ± 24
1.00	−27.23 ± 2.7	−45.00 ± 8.9	−1607.5 ± 9.4	330 ± 20

[a] Uncertainties are standard errors of the coefficients in least-squares $\Delta G^0 = \Delta H^0 - \Delta S^0 T$ refinement.

[b] Estimated errors (95% confidence) are cumulative values based on uncertainties in the ΔG^0–T refinement and the reference data.

dissociative chemisorption during Step 1 and formation of hydrous oxide or hydrate during Step 2. In Step 3 and beyond, ΔG^0_{298} becomes increasingly insensitive to sorption of additional water and asymptotically approaches −8.56 kJ mol^{-1}, the ΔG^0_{298} for $H_2O(g) \rightarrow H_2O(l)$ [14]. ΔH^0_{298} for sorption beyond Step 2 should be near the theoretical value (−44 kJ mol^{-1}) for condensation of water, as observed for the single reversible desorption in closed-system tests [12].

Thermal desorption of water is anticipated in two distinct temperature ranges. Loss of weakly bound H_2O from Step 3 and beyond is expected near the 373 K boiling point of water. Extrapolation of $\underline{G}$–T data (Table 1) for median (y = 0.5, n = 0.5) compositions of Steps 1 and 2 show that equilibrium pressures for both terminal products reach 1 bar near 575 K, the expected point for onset of a second desorption. These predictions agree with observations of Stakebake [11], but not with those of Paffett et al. [12] who describe a single reversible desorption of all water in the 350–500 K range during closed-system measurements. Comparison of enthalpies for Steps 1 and 2 (−41 and −27 kJ mol^{-1} H_2O) and that (285 kJ mol^{-1}) for removing strongly bound water [11] shows that desorption is activated (irreversible). Sorption in Step 3 and beyond is non-activated and reversible.

Paffett et al. attribute the absence of an inflection point in adsorbate concentration-P_{H_2O} data to an insignificant difference between enthalpies of monolayer and multilayer sorption [12]. All water added to the closed-system participated in reversible sorption–desorption cycles at 295–525 K, but strongly bound water was not involved because the desorption temperatures for Steps 1 and 2 extend well beyond 600 K at 10-bar H_2O overpressure. The unspecified temperatures used to dry oxide samples were apparently inadequate for removing water of Steps 1 and 2 prior to the measurements.

Residual water is of concern for extended PuO_2 storage [2,3,10]. Elimination of H_2O from PuO_2 by heating to 500 K is claimed by Paffett et al. [12], but that temperature is inadequate for reversing Steps 1 and 2. Calcining above 1200 K [3] is required because a mass loss of uncertain origin occurs upon heating of water-exposed oxide at 1000–1200 K [11]. Progressive and irreversible mass gains during repeated cycles of water exposure at 303 K and heating at 373 K [8] is consistent with reaction of water and dioxide to form PuO_{2+x} [5], but decomposition of that product is expected below 1000 K [15]. Re-sorption of water after firing is possible because calcined oxide extracts moisture from other surfaces, as well as from desiccants such as $CaCl_2$. Use of procedures that slow the sorption rate appears more effective for limiting water uptake by calcined oxide than maintenance of atmospheres with sufficiently low water concentrations [13].

Kim and Kanellakopulos [6] suggest that dioxide solubility is enhanced by formation of a more soluble (less stable) surface hydroxide like PuO_2(hyd) [14]. $Pu(OH)_4^0$(aq) is the only significant solution species at chemical potentials of near-neutral solutions [16]. Respective equilibrium $Pu(OH)_4^0$ concentrations calculated for $PuO(OH)_2$ (ads, surf), PuO_2(cr), and PuO_2-(hyd) at pH 7 using reference data [14,17] and results in Table 2 are 2×10^{-19}, 3×10^{-17}, and 3×10^{-11} M. Inclusion of possible surface energy effects using data for $Ca_3Si_2O_7$ [18] shows that $PuO(OH)_2$ may be destabilized by as much as 30 kJ mol^{-1} and that oxide solubility may increase to 4×10^{-14} M. The derived surface energy is considered bounding because the basicity of

$(CaO)_3 \cdot (SiO_2)_2$ most likely exceeds that of PuO_2. A problem remains even if PuO_2(cr) surfaces are somehow transformed to PuO_2(hyd). The observed steady-state [Pu] ($\sim 1 \times 10^{-7}$ M at pH 7) is 10^3–10^4 greater than predicted for hydrous oxide and the primary (>95%) oxidation states at steady-state are Pu(V) and Pu(VI), not Pu(IV) [16]. These are serious discrepancies that merit attention.

4. Conclusions

Derived Gibbs energies are consistent with step-wise chemisorption of two irreversibly bound water layers and physisorption of additional layers of reversibly bound water. Results support a two-step thermal desorption process. Application of the findings to oxide storage and solubility show that perplexing and unresolved issues remain.

References

[1] J.M. Haschke, R.G. Haire, in: D. Hoffman (Ed.), Advances in Plutonium Chemistry, American Nuclear Society, La Grange Park, IL, 2002, p. 212 (Chapter 9).
[2] J.M. Haschke, J.C. Martz, in: R.A. Meyers (Ed.), Encyclopedia of Environmental Analysis and Remediation, John Wiley and Sons, New York, 1998, p. 3740.
[3] U.S. Department of Energy Standard; Stabilization, Packaging, and Storage of Plutonium-Bearing Materials, DOE-STD-3013-2000, US Department of Energy, Washington, DC, 2000.
[4] J.M. Haschke, T.H. Allen, L.A. Morales, J. Alloys Compd. 314 (2001) 78.
[5] J.M. Haschke, T.H. Allen, L.A. Morales, Science 287 (2000) 285.
[6] J.I. Kim, B. Kanellakopulos, Radiochim. Acta 48 (1989) 145.
[7] J.D. Moseley, R.O. Wing, Properties of Plutonium Dioxide, Report RFP-503, Rocky Flats Plant, The Dow Chemical Company, Golden, CO, August 1665.
[8] J.L. Stakebake, M.L. Steward, J. Colloid Interface Sci. 42 (1973) 328.
[9] H. Benhamou, J.P. Beraud, Analysis A 8 (1980) 376.
[10] J.M. Haschke, T.E. Ricketts, J. Alloys Compd. 252 (1997) 148.
[11] J.L. Stakebake, J. Phys. Chem. 77 (1973) 581.
[12] M.T. Paffett, D. Kelly, S.A. Joyce, J. Morris, K. Veirs, J. Nucl. Mater. 322 (2003) 45.
[13] J.M. Haschke, T.E. Ricketts, Plutonium Dioxide Storage: Conditions for Preparation and Handling, Report LA-12999-MS, Los Alamos National Laboratory, Los Alamos, NM, August 1995.
[14] J. Fuger, H. Nitsche, P. Potter, M.H. Rand, J. Rydberg, K. Spahiu, J.C. Sullivan, W.J. Ullman, P. Vitorge, H. Wanner, Chemical Thermodynamics of Neptunium and Plutonium, Elsevier, Amsterdam, 2001, p. 53.
[15] J.M. Haschke, T.H. Allen, J. Alloys Compd. 336 (2002) 124.
[16] J.M. Haschke, R.L. Bassett, Radiochim. Acta 90 (2002) 505.
[17] D. Langmuir, Aqueous Environmental Geochemistry, Prentice-Hall, Upper Saddle River, New Jersey, 1997, p. 557.
[18] S. Braunauer, Adv. Chem. Ser. 33 (1961) 5.